

pubs.acs.org/acscatalysis Research Article

Bimetallic Mechanism for Alkyne Cyclotrimerization with a Two-Coordinate Fe Precatalyst

Ryan J. Witzke, Diptarka Hait, Khetpakorn Chakarawet, Martin Head-Gordon, and T. Don Tilley*



Cite This: ACS Catal. 2020, 10, 7800-7807



ACCESS

III Metrics & More

Article Recommendations

Supporting Information

ABSTRACT: The two-coordinate compound (IPr)Fe[N(SiMe₃)-DIPP] (IPr = 1,3-bis(2,6-diisopropylphenyl)imidazolin-2-ylidene; DIPP = 2,6-diisopropylphenyl) catalyzes the cyclotrimerization of alkynes to arenes. Treatment of the Fe complex with 1 equiv of diphenylacetylene results in the formation of a bimetallic bridging alkyne complex, along with dissociation of IPr from Fe. At elevated temperatures, the bridging alkyne complex undergoes oxidative coupling to form a dimetallacyclopentadiene complex, formally by a one-electron oxidation at each metal center. Each complex catalyzes



the cyclotrimerization of diphenylacetylene. Kinetic studies exhibit first-order dependence on the bimetallic complexes, providing further support for the presence of these species in the catalytic cycle. DFT calculations support the experimental mechanistic data and suggest that the catalytic cycle is completed by binding of an alkyne to the diene complex, followed by insertion to form a hexatriene species that then undergoes ring closure to form an inverse sandwich complex, $[DIPP(Me_3Si)N]Fe(\eta^6-arene)Fe[N(SiMe_3)DIPP]$. The arene product is then displaced by alkyne to close the catalytic cycle.

KEYWORDS: catalysis, two-coordinate, bimetallic, mechanism, alkyne cyclotrimerization

■ INTRODUCTION

First-row transition-metal complexes have attracted increasing attention as catalysts, since base metals are more abundant and more cost effective relative to the analogous second- and third-row metal compounds. The development of catalysts with the lighter metals poses an interesting challenge, given the different properties expressed by such metal centers, including their tendency toward high-spin configurations and one-electron-redox processes. In general, these characteristics necessitate unique elementary transformations for substrate activations and catalytic turnover, many of which have yet to be defined.

Studies from this laboratory have focused on open-shell, twocoordinate first-row metal complexes and the establishment of fundamental reaction steps that may be incorporated into catalytic cycles.³⁻¹¹ For example, the two-coordinate Ni complex $Ni[N(SiMe_3)DIPP]_2$ (DIPP = 2,6-diisopropylphenyl) was observed to catalyze C-C cross-coupling reactions and undergo well-defined one-electron-redox processes that account for catalysis. 10 Stoichiometric reactivity studies allowed isolation of kinetically competent intermediates and definition of a detailed mechanism that features a number of one-electron redox steps involving Ni(I), Ni(II), and Ni(III). This mechanism differs from that associated with palladium-catalyzed couplings, which involve classic two-electron oxidative additions. The higher propensity of nickel vs palladium to undergo one-electron transformations has considerable precedent, but more research is needed to better define the reaction steps generally available to first-row metal complexes. 10,12

The viability of catalysis by open-shell two-coordinate complexes has been demonstrated by only a small number of additional examples, including hydrosilylations of olefins/ketones, 6,13 cyclotrimerizations of alkynes/isocyanates, 8,14 and reduction of dinitrogen to ammonia, 15 all of which lack significant mechanistic information. The cyclotrimerization of alkynes, catalyzed by the Fe(I) complex (IPr)Fe[N(SiMe₃)-DIPP]⁸ (1, Scheme 1) (IPr = 1,3-bis(2,6-diisopropylphenyl)-imidazolin-2-ylidene), seemed to represent an interesting case

Scheme 1. Previous Results Showing the Capacity of 1 as a Catalyst for Alkyne Cyclotrimerization

$$R = Me, R' = Me: R' = Me = Me, R' = Ph: R' = Me, R' = H: 80\%$$

Received: April 24, 2020 Revised: June 15, 2020 Published: June 18, 2020





for study, since mechanisms for this reaction type have received considerable attention and are generally believed to proceed via two-electron reductive couplings and metallocyclopentadiene intermediates (Scheme 2).

Scheme 2. Mechanisms for Alkyne Coupling

The history of alkyne cyclotrimerization dates back to 1948, when Reppe first reported the trimerization of acetylene to benzene catalyzed by a Ni(II) complex. Since then, this reaction has been significantly expanded upon in terms of both catalysts and substrates. Its maturation has led to its use in the synthesis of several natural products. Substituted aromatic rings are commonly found in nature; thus, this reaction should still have significant applications in the future.

As shown in Scheme 2, the generally accepted mechanism for alkyne cyclotrimerization involves coordination of two alkynes to the metal, followed by coupling to form a metallacyclopentadiene complex. The latter intermediate then coordinates and inserts another alkyne to form the arene product. 17,32 The possibility of a two-electron coupling at Fe(I) to produce an Fe(III) metallacyclopentadiene was particularly interesting, since it would seem to represent a two-electron process for a first-row metal. This contribution describes experimental and computational work showing that this coupling actually corresponds more closely to a one-electronredox process at Fe(I) and the cooperative participation of two metal centers results in formation of a diene intermediate (Scheme 2). Other mechanisms involving two metals have been suggested (Scheme 2), but all proceed through unsymmetrical binding of the bimetallacyclopentadiene fragment, resulting in a two-electron oxidation at one metal while the other metal coordinates to the π system of the resulting diene. ^{33–36} The results presented here provide important mechanistic information regarding fundamental steps that are possible for first-rowmediated transformations, with implications for how new catalytic coupling processes may be designed.

■ RESULTS AND DISCUSSION

Synthesis and Characterization of Potential Catalytic Intermediates. While complex 1 exhibits good catalytic efficiency, the identity and structure of intermediates in this system were unknown. Previous catalytic reactivity reported from this laboratory employed 2-butyne, 1-phenyl-1-propyne, and 3-methyl-1-butyne as substrates; however, the isolation of possible intermediates with stoichiometric quantities of these substrates proved unsuccessful due to rapid catalytic turnover (Scheme 1).8

In order to access a slower trimerization more amenable to a mechanistic study, the sterically demanding alkyne diphenylacetylene was examined. For this substrate, the rate of catalytic coupling by 1 was significantly reduced such that elevated temperatures were required for formation of hexaphenylbenzene (ca. 60 °C). More interestingly, the reaction mixture changed from red to orange-brown upon addition of the alkyne to 1 in toluene. This suggested the presence of a new alkyne-iron complex, and in pursuit of this 1 was treated with 1 equiv of diphenylacetylene to afford the bimetallic bridged bis(alkyne) complex $\{[DIPP(Me_3Si)N]Fe(\mu,\eta^2-PhCCPh)\}_2$ (2), along with unbound IPr (eq 1). Due to the similar solubility properties

of IPr and 2, removal of IPr from the reaction mixture proved difficult; however, this separation was effected by introduction of 1 atm of CO_2 to remove IPr from the reaction mixture via formation of the toluene-insoluble CO_2 –IPr adduct.³⁷ Filtration, followed by crystallization from minimal toluene cooled to $-35~^{\circ}C$, afforded 2 in 41% yield.

Characterization of **2** by single-crystal X-ray diffraction (Figure 1) reveals an elongated alkyne C–C bond (1.316(6) Å) relative to that of free diphenylacetylene $(1.204(2) \text{ Å}^{38})$.

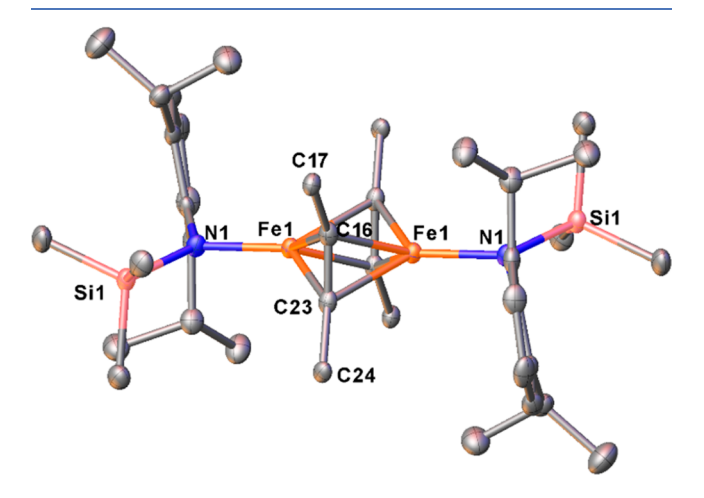


Figure 1. Solid-state structure of **2** shown with thermal ellipsoids at 50% probability. Most of the phenyl groups and all hydrogen atoms have been omitted for clarity.

Consistently, the coordinated alkyne is bent, with an average C–C–C_{phenyl} bond angle of 142.7°. In the 13 C{ 1 H} NMR spectrum, a resonance corresponding to the bridging alkyne carbons was observed at 110 ppm, which is downfield relative to the corresponding shift for free diphenylacetylene (89 ppm) and upfield of that for stilbene (137 ppm). These observations can be attributed to π back-bonding of Fe electron density into the π^* orbitals of the alkyne. Complex 2 is diamagnetic, presumably due to antiferromagnetic coupling as a result of either direct overlap of the metal molecular orbitals or superexchange occurring through the alkyne π system.

The loss of IPr during complexation of 1 with diphenylacetylene was unexpected, given its well-established σ -donor properties. The driving force for this ligand exchange is presumed to be associated with the superior π acidity of the alkyne ligands that stabilize 2 in the formally low (+I) oxidation state. In addition, the high steric demands of IPr may facilitate its dissociation. We propose that an initial association of alkyne to an open coordination site in 1 promotes rapid IPr dissociation, followed by dimerization to form 2; however, it is not known whether the dissociation and dimerization occur in sequence or in a concerted fashion. Attempts to study the kinetics of this process by UV—vis spectroscopy were unsuccessful due to the rapid rate of the reaction.

Heating complex **2** to 60 °C resulted in coupling of the alkynes to form a dimetallacyclopentadiene complex, {[DIPP- $(Me_3Si)N]Fe}_2(\mu,\kappa^2-C_4Ph_4)$ (3, in 46% isolated yield), in which each of the Fe atoms have been oxidized by one electron (formally to Fe(II), eq 2). Complex **3** has a temperature-

dependent magnetic moment (approximately 2.72 $\mu_{\rm B}$ at room temperature) on account of weak antiferromagnetic coupling between the two Fe(II) centers (see the Supporting Information). Magnetic susceptibility data for 2 were fitted to the Heisenberg–Dirac–van Vleck exchange Hamiltonian $-2J\overline{S_1}$, $\overrightarrow{S_2}$, where J is the coupling constant. Fitting to the experimental data gives $J=-70~{\rm cm}^{-1}$, which is in reasonable agreement with a density functional theory (DFT) estimate of $J=-80~{\rm cm}^{-1}$ for the simpler model system $\{{\rm Ph}({\rm H_3Si})\}{\rm Fe}\}_2(\mu,\kappa^2-{\rm C_4Me_4})$. The X-ray structure reveals two distinct sets of dienyl C–C bond distances: C1–C2 = C3–C4 = 1.399(2) Å and C2–C3 = 1.497(2) Å, which correspond to double and single bonds, respectively (Figure 2). A similar symmetric dimetallacyclopentadiene Ta complex was recently reported, but was not studied as a catalyst for alkyne cyclotrimerization.

Presumably, the large steric profile of the phenyl groups of the alkyne ligand stabilizes complex **2**, which then requires elevated temperatures for coupling to form **3**. In contrast, treatment of **1** with 1 equiv of 3-hexyne, at ambient temperature, resulted in the isolation of {[DIPP(Me₃Si)N]Fe}₂(μ , κ ²-C₄Et₄) (**4**), without observation of the bis(alkyne) intermediate (by ¹H NMR spectroscopy) (eq 3). Analogously to **3**, this complex has a magnetic moment of 2.87 μ _B and a similar connectivity was confirmed by X-ray diffraction (Figure S5 in the Supporting Information).

⁵⁷Fe Mössbauer Data for 2 and 3. The zero-field ⁵⁷Fe Mössbauer spectrum of compound 2 displays a Lorentzian

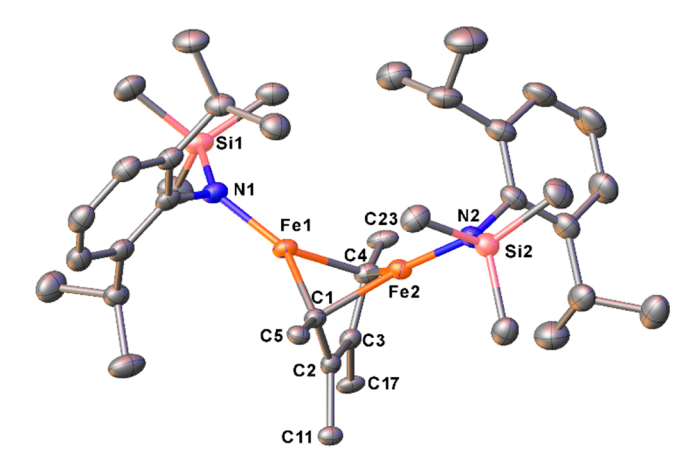


Figure 2. Solid-state structure of **3** shown with thermal ellipsoids at 50% probability. Most of the phenyls, a molecule of diethyl ether, and all hydrogen atoms have been omitted for clarity.

doublet with an isomer shift of 0.388(2) mm/s and a quadrupole splitting of 1.678(4) mm/s at 5 K, while that of 3 exhibits an isomer shift of 0.483(1) mm/s and a quadrupole splitting of 2.183(3) mm/s (Figure 3). Even though, to the best of our

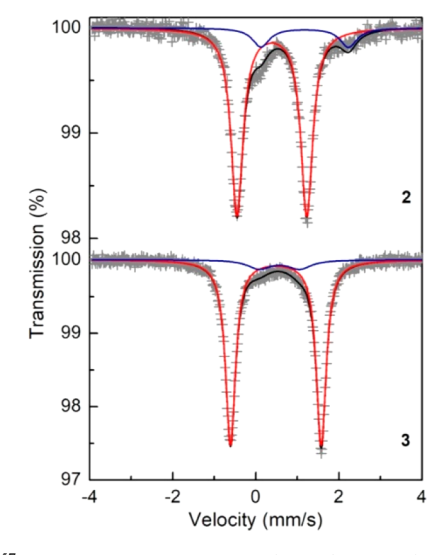


Figure 3. ⁵⁷Fe Mössbauer spectra of **2** (upper) and **3** (lower) at 5 K. Red lines represent the respective compounds, blue lines are minor impurities, and black lines are the total fit.

knowledge, no similar Fe compounds exist in the literature with Mössbauer analysis, the isomer shifts of **2** and **3** are comparable to those of other low-coordinate Fe complexes.^{8,41,42}

The lower isomer shift of **2** in comparison to that of **3** suggests that the Fe centers in the alkyne complex possess less electron density, which may be attributed to the alkyne's ability to accept electron density via π back-bonding. On the other hand, the diene's π^* orbitals in compound **3** are not accessible to the Fe for π back-bonding due to the geometrical constraint. It should be noted, however, that a similar trend in the change in isomer

shifts was observed for the two-coordinate Fe(I/II) system and may be attributed to an increase in 4s-3d mixing for Fe(I) complexes. The appearance of only one doublet in the Mössbauer spectrum of 3 is consistent with symmetric oxidative coupling of the alkynes, with each Fe being oxidized by one electron.

Catalytic Activity and Kinetics. Complexes 2 and 3 both catalyze the cyclotrimerization of diphenylacetylene at 70 $^{\circ}$ C in the absence of IPr. A kinetic study was performed to probe the mechanism of alkyne cyclotrimerization with this system using the conditions shown in Scheme 3. Complex 4 was used because

Scheme 3. General Reaction Conditions Used for All Kinetic Runs

the resulting product, hexaethylbenzene, was significantly more soluble than the product (hexaphenylbenzene) from catalysis with 2 or 3. The order in [4] was determined by initial rate measurements using varying concentrations of 4, while the concentration of 3-hexyne was held constant at 0.342 M in THF- d_8 . The results, plotted in Figure 4, confirm that the catalysis is first order in [4] and are consistent with the presence of bimetallic species in the catalytic cycle.

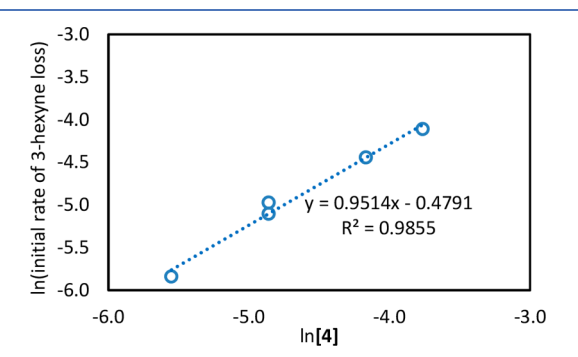


Figure 4. log/log plot exhibiting first-order dependence in 4.

An analogous series of experiments with varying alkyne concentration at a constant [4] of 7.76×10^{-3} M revealed a first-order dependence on [3-hexyne] (Figure 5). This, in combination with the knowledge that 4 forms at room temperature and only catalyzes the formation of arene at

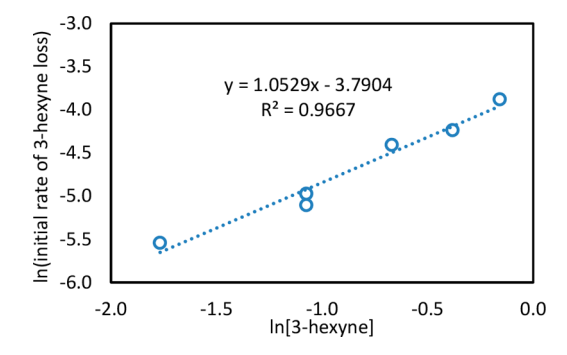


Figure 5. log/log plot exhibiting first-order dependence in 3-hexyne.

elevated temperatures, indicates that the rate-determining step is associated with addition of the final alkyne. The presence of both 3 and 4 during catalysis was observed by ¹H NMR spectroscopy.

To determine the effect of IPr and hexaethylbenzene concentrations on catalysis, additional kinetic experiments were performed. The initial rate of 3-hexyne consumption with catalyst 4 in the presence of 20 equiv of IPr was $[6.4(1)] \times 10^{-3}$ M min⁻¹, which is very close to the rate without IPr $([6.1(1)] \times 10^{-3}$ M min⁻¹) (Figure 6). The lack of a significant

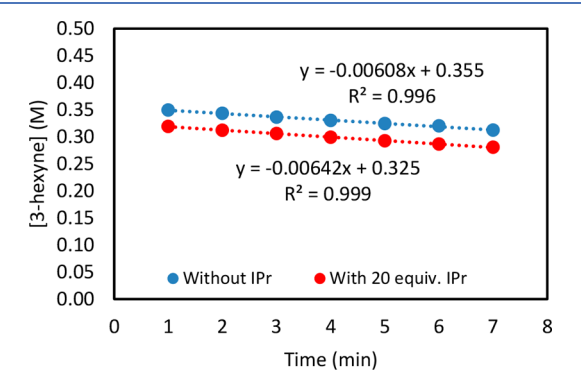


Figure 6. Kinetic profile of 3-hexyne cyclotrimerization catalyzed by 4 with (red) and without (blue) added IPr. There is no effect of [IPr] on the rate of catalysis.

difference between these values indicates that catalysis is essentially unaffected by the presence of IPr. Rapid and irreversible IPr decoordination from 1 likely occurs under catalytic conditions, which further supports the hypothesis that 1 is a precatalytic species and that IPr does not compete effectively with alkyne as a ligand for the Fe center.

On the other hand, the concentration of hexaethylbenzene dramatically affects the rate of catalysis. As can be seen in Figure 7, both the total conversion and the rate of reaction are lower in

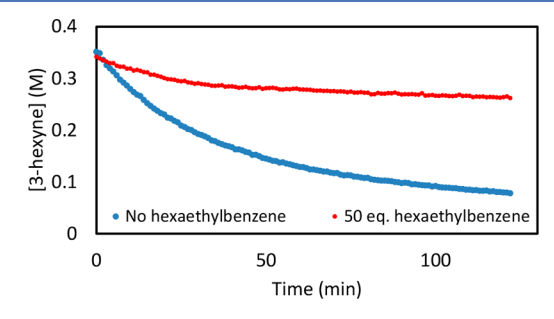


Figure 7. Plot of concentration of 3-hexyne over time with (red) and without (blue) 50 equiv of hexaethylbenzene.

the presence of 50 equiv of hexaethylbenzene, indicating significant product inhibition. The presence of the product in solution likely slows the rate of arene dissociation. Moreover, catalytic inhibition increases with product formation over the course of the reaction, and for this reason initial rates were used for kinetic analysis.

Several attempts were made to obtain intermediates formed upon addition of the third alkyne. Treatment of **3** or **4** with stoichiometric quantities of diphenylacetylene, 3-hexyne, or bis(trimethylsilyl)acetylene resulted in either no reaction or formation of an arene product, depending on the temperature. Additionally, **1** was treated with CO₂ while it was dissolved in mesitylene in the hope that IPr-CO₂ would form in addition to

ACS Catalysis pubs.acs.org/acscatalysis Research Article

an inverse arene sandwich complex; however, only decomposition occurred.

From the above results, a mechanism can be proposed (Scheme 4). The first-order dependence in [4] indicates that the

Scheme 4. Proposed Mechanism for Arene Formation^a

 a Calculated structures (with $-N(SiH_{3})Ph$) are indicated by labels from Figure 8.

catalysis proceeds through bimetallic intermediates and implies some electronic cooperation between the two Fe centers. The first-order dependence on [3-hexyne] in its reaction with 4 is consistent with incorporation of the third alkyne in the rate-determining step and with the requirement of elevated temperatures for product formation. The lack of a dependence on [IPr] means that, once displaced by alkyne, the NHC does not participate in the reaction. Since these studies provide no information regarding intermediates that result from addition of the final alkyne to the dimetallacyclopentadiene intermediate, a

DFT investigation was carried out to address this aspect of the mechanism.

Mechanistic Density Functional Theory. Density functional theory (DFT) calculations (with the ωB97X-V functional)⁴³ were carried out to determine potential mechanistic pathways for cyclotrimerization and to estimate approximate barrier heights. A simplified model system where the DIPP-(Me₃Si)N- ligand is replaced by Ph(H₃Si)N- was chosen for computational efficiency and employed 2-butyne as the alkyne. The reported free energies were computed via ensemble averaging over all available spin states, in order to account for potential crossovers from the observed antiferromagnetic coupling to any ferromagnetic regime. Further details about the DFT calculations are supplied in the Supporting Information

The ΔG value for formation of the bimetallic bridging bis(alkyne) complex { $[Ph(H_3Si)N]Fe(\mu,\eta^2-MeCCMe)$ }₂ (A) from the monomeric $[Ph(H_3Si)N]Fe(\eta^2-MeCCMe)$ (M1) is -20.6 kcal/mol at room temperature. Similarly, ΔG for the formation of A from the monoiron bis(alkyne) [Ph(H₃Si)N]- $Fe(\eta^2\text{-MeCCMe})_2$ (M2) complex is -20.4 kcal/mol. These results suggest that the bimetallic complex A is quite thermodynamically stable relative to potential monometallic species, and therefore the concentration of any such monometallic species will be both extremely small and scale as the square root of the concentration of bimetallic species. A catalytic route involving a single Fe center therefore should have kinetics that scale as the square root of the concentration of bimetallic species, unlike the first-order kinetics observed experimentally. This suggests that the bimetallic species itself is involved in the catalysis.

Next, the routes to cyclotrimerization from **A** were investigated (Figure 8). This mechanism begins with **A** undergoing alkyne coupling to form a dimetallacyclopentadiene complex, $\{[Ph(H_3Si)N]Fe\}_2(\mu,\kappa^2-C_4Me_4)$ (**B**), analogous to the conversion of **2** to **3**. The barrier for this step appears to be

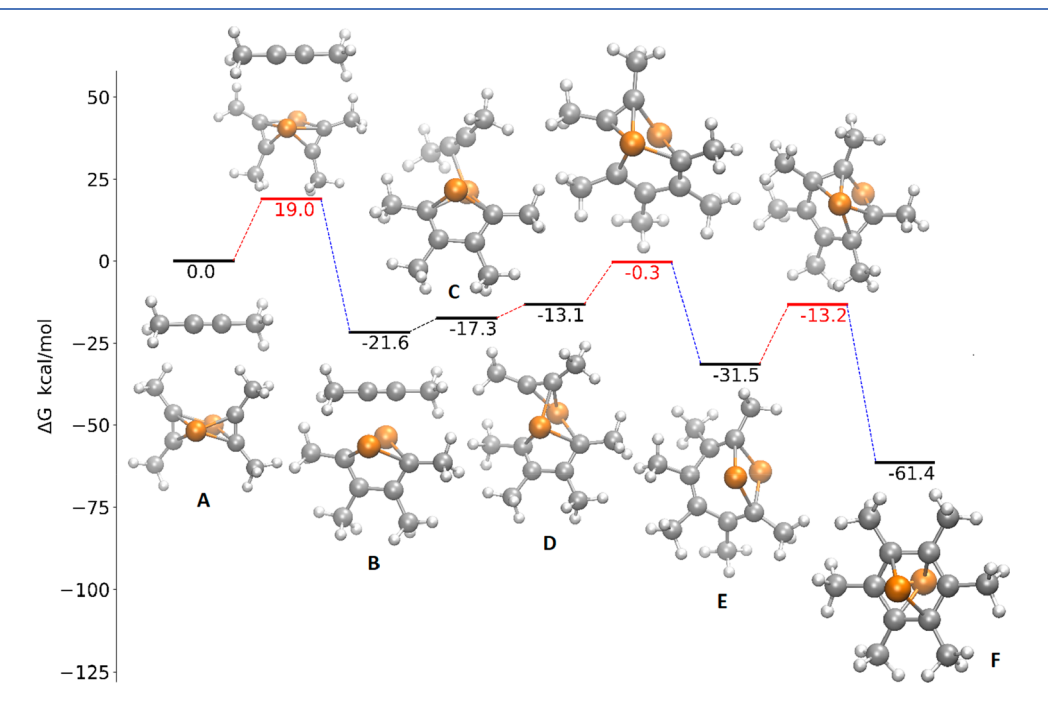


Figure 8. Calculated mechanism for cyclotrimerization of 2-butyne by Fe[N(SiH₃)Ph] (amido ligands omitted for clarity).

fairly high at ΔG^{\ddagger} = 19.0 kcal/mol, though **B** is more stable than **A** by 21.6 kcal/mol in ΔG .

An alkyne molecule subsequently attaches to a single Fe center in **B** to generate $\{[Ph(H_3Si)N]Fe(\eta^1-MeCCMe)\}(\mu,\kappa^2-MeCCMe)\}$ C_4Me_4 {Fe[N(SiH₃)Ph]} (C). The formation of C from B and an alkyne appears to be barrierless, though a small barrier is possible in the actual system due to disruption of dispersion interactions between DIPP groups. The added alkyne then migrates to become a bridging ligand between the two Fe centers, forming $\{[Ph(H_3Si)N]Fe\}_2(\mu,\kappa^2-C_4Me_4)(\mu,\eta^2-C_4Me_4)$ MeCCMe) (D). Transition structure searches along the coordinate connecting C and D seemed to converge to structures quite close to D, both geometrically and energetically, suggesting that D is a shallow minimum very close to the transition state of formation. The relatively small free energy gap between D and C (4.2 kcal/mol) also seems to suggest that D could directly form from B and 2-butyne without the formation of intermediate C.

The bridging alkyne in **D** subsequently inserts into the diene to form a dimetallacycloheptatriene complex, $\{[Ph(H_3Si)N]-Fe\}_2(\mu,\kappa^2-C_6Me_6)$ (E). The barrier for this insertion is 12.9 kcal/mol, indicating a fast turnover at room temperature (half-life of milliseconds from transition state theory). An attempt was also made to find a transition structure for a Diels–Alder type process for simultaneous formation of two C–C bonds between the alkyne and the diene, but no such transition structure could be found

Finally, the dimetallacycloheptatriene complex E undergoes ring closure to form $\{[Ph(H_3Si)N]Fe\}_2(\mu,\eta^6-C_6Me_6)$ (F), which contains the C₆Me₆ arene moiety sandwiched between the two iron centers. This step has a fairly high activation barrier $(\Delta G^{\ddagger} = 18.3 \text{ kcal/mol})$ presumably due to the significant weakening of the Fe-C bonds in the transition structure and the considerable geometrical distortion of the dimetallacycloheptatriene ring to bring the two carbons closer to their final bond length of 1.45 Å from their initial separation of 3.23 Å (the transition state distance is 2.34 Å). A recent report by the Tsai group fully isolated and characterized a similar chromium-based inverse sandwich complex, which is a competent catalyst for alkyne cyclotrimerization.⁴⁴ It is also worth noting that F has weak ferromagnetic coupling between the Fe centers (unlike the antiferromagnetic coupling hereto observed), presumably on account of either greater separation between Fe centers or weak superexchange via the sandwiched arene.

The cycle concludes with release of arene from F. This could entail addition of alkyne to the Fe centers in F, followed by subsequent detachment of M1. The energetics of this process were examined, and they all appear to be barrierless, rendering the exercise to be nontrivial. ΔG for the first alkyne addition was -6.6 kcal/mol and -1.5 kcal/mol for the second, indicating that these are unlikely to slow down the overall catalysis. The detachment of the first M1 moiety has an associated ΔG of -2.5kcal/mol, and the detachment of the second requires a ΔG of -1.4 kcal/mol. These small values are a consequence of a positive ΔH from loss of the Fe-arene interactions being countered by entropic gains from one large species dissociating into two smaller entities. Thus, the free energy barrier to dissociation is unlikely to be any greater than the ΔH values, which are 12.8 and 15.7 kcal/mol, respectively. Since these are smaller than the barriers for formation of B and F, the dissociation of the arene is not likely to be the rate-determining step. Excess arene can nonetheless slow down catalysis by

competing with the alkyne for binding to the metal and thereby shifting the equilibrium.

It is worth noting that the mechanism in Figure 8 predicts that the step with the highest barrier is the formation of B, which is not consistent with the experimental kinetic data which indicate that the rate determining step occurs subsequent to addition of the third alkyne. However, the calculated barriers for formation of **B** and **F** are very close (19.0 and 18.3 kcal/mol, respectively). Errors on the scale of 1 kcal/mol are quite standard in DFT calculations for main-group-chemistry barrier heights, 45,46 and transition metals are typically far more challenging. 47 We also note that the smaller size of N(SiH₃)Ph vs N(SiMe₃)DIPP could conceivably alter the computed barriers via differences in noncovalent ligand—ligand interactions in the bimetallic species. Specifically, the ring-closing step leading to the formation of F involves a significant increase in the Fe-Fe distance (from 2.7 to 3.5 Å) and thus likely leads to a significant loss of ligand-ligand dispersion stabilization. A rough analysis of this effect (see Section 8 of the Supporting Information) indicates that the barrier of the ring-closing step increases by 1 kcal/mol when the full N(SiMe₃)DIPP ligand is employed (leading to an estimated barrier of ~19 kcal/mol barrier for formation of the sandwich complex). Similarly, it appears that formation of B leads to a strengthening of ligand-ligand interactions, which leads to a lowering of the barrier for that step by ~1 kcal/mol when N(SiMe₃)DIPP is present instead of N(SiH₃)Ph (leading to an estimated barrier of ~18 kcal/mol). This effect indicates that the ring-closing step is the highest barrier process (and thus the ratedetermining step), as indicated by the experimental system. Therefore, a combination of intrinsic DFT error and differences between ligand-ligand interactions in the model and experimental systems can easily justify this apparent disagreement between theory and experiment. As a result, it seems very likely that the ring closure step to form the analogue of F is the true rate-determining step of the cycle.

Proposed Mechanism. As described in Scheme 2, there are various pathways known for bimetallic alkyne cyclotrimerization: (a) an alkyne coordinates between two metals in a bimetallic framework followed by insertion of another alkyne into the M-C bond, (b) one alkyne coordinates to each metal followed by oxidative coupling to form the dimetallacyclopentadiene, and (c) a metallacyclopentadiene is formed entirely on one metal center, and then the other metal coordinates to the diene via the π system.³³ The isolation of intermediates 2–4 led us to the possibility of a new mechanism distinct from the monometallic and bimetallic mechanisms known in the literature, which generally involve a two-electron-oxidation step to form a metallacyclopentadiene. The oxidative coupling to form 3 from 2 divides the two-electron process over two metals, resulting in a formal one-electron oxidation at each metal to generate the Fe(II)Fe(II) dimer instead of a mixed-valent Fe(I)Fe(III) complex. The Mössbauer data corroborate this, as the appearance of only one doublet in the spectrum for 3 implies that each Fe is equivalent.

On the basis of the bimetallic complexes synthesized, and by mechanistic DFT calculations, we propose a new pathway in which two alkynes first coordinate in a μ - η^2 fashion to form 2. Subsequent oxidative alkyne coupling occurs to form the symmetric dimetallacyclopentadiene complex 3 (or 4). A third equivalent of alkyne subsequently coordinates to 3, followed by insertion to form a dimetallacycloheptatriene complex. This complex couples to afford an inverse sandwich complex, which then coordinates alkyne and releases arene as the product.

■ CONCLUDING REMARKS

This work provides evidence for a new mechanism for bimetallic alkyne cyclotrimerization (Scheme 4). The cooperation between the two metals during the oxidative coupling to form 3 from 2 results in a formal one-electron oxidation at each metal. This aspect of the transformation is consistent with what has previously been reported for two-coordinate catalysts and further supports the idea that low-coordinate catalysts tend to act through one-electron steps. Furthermore, the metal—metal interaction in this work may have applications toward the goal of developing earth-abundant 3d transition-metal catalysts capable of performing two-electron processes through bimetallic cooperativity. 48,49

ASSOCIATED CONTENT

Supporting Information

The Supporting Information is available free of charge at https://pubs.acs.org/doi/10.1021/acscatal.0c01828.

Additional experimental procedures, crystallographic data, spectral characterization, and DFT details (PDF)

Computed structures (ZIP)

Crystallographic data (CIF)

Crystallographic data (CIF)

Crystallographic data (CIF)

AUTHOR INFORMATION

Corresponding Author

T. Don Tilley — Department of Chemistry, University of California, Berkeley, Berkeley, California 94720, United States; orcid.org/0000-0002-6671-9099; Email: tdtilley@berkeley.edu

Authors

Ryan J. Witzke — Department of Chemistry, University of California, Berkeley, Berkeley, California 94720, United States; o orcid.org/0000-0003-1729-1636

Diptarka Hait — Department of Chemistry, University of California, Berkeley, Berkeley, California 94720, United States; orcid.org/0000-0003-1570-920X

Khetpakorn Chakarawet — Department of Chemistry, University of California, Berkeley, Berkeley, California 94720, United States; orcid.org/0000-0001-5905-3578

Martin Head-Gordon — Department of Chemistry, University of California, Berkeley, Berkeley, California 94720, United States; orcid.org/0000-0002-4309-6669

Complete contact information is available at: https://pubs.acs.org/10.1021/acscatal.0c01828

Author Contributions

The manuscript was written through contributions of all authors. All authors have given approval to the final version of the manuscript.

Funding

This work was funded by the NSF under grant no. CHE-1954808. We acknowledge the NIH (grant nos. SRR023679A and 1S10RR01663401) and NSF (grant no. CHE-0130862) for funding of the College of Chemistry NMR facility (UC, Berkeley). X-ray analysis of **2**–**4** were performed at the ChexRay crystallographic facility (UC, Berkeley), which is funded by the NIH under grant no. S10RR027172. The computational work was supported by the Director, Office of Science, Office of Basic

Energy Sciences, of the U.S. Department of Energy under Contract No. DE-AC02-05CH11231.

Notes

The authors declare no competing financial interest.

ACKNOWLEDGMENTS

We thank Professor Christopher J. Chang at UC Berkeley for the use of the Mössbauer spectrometer. We also thank Dr. Michael Lipschutz for the data collection and initial solution of the X-ray crystal structure of **2**. CIF files can also be obtained free of charge from the Cambridge Crystallographic Data Centre under reference numbers 2009604, 2009605, and 2009606.

REFERENCES

- (1) Catalysis Without Precious Metals; Bullock, R. M., Ed.; Wiley-VCH: Weinheim, 2010, 1.
- (2) van Leest, N. P.; Epping, R. F. J.; van Vliet, K. M.; Lankelma, M.; van den Heuvel, E. J.; Heijtbrink, N.; Broersen, R.; de Bruin, B. Single-Electron Elementary Steps in Homogeneous Organometallic Catalysis, 1st ed.; Elsevier: 2018; Vol. 70, p 71.
- (3) Cai, I. C.; Lipschutz, M. I.; Tilley, T. D. A Bis(Amido) Ligand Set That Supports Two-Coordinate Chromium in the + 1, + 2, and + 3 Oxidation States. *Chem. Commun.* **2014**, *50*, 13062–13065.
- (4) Liu, H.-J.; Cai, I. C.; Fedorov, A.; Ziegler, M. S.; Copéret, C.; Tilley, T. D. Tricoordinate Organochromium(III) Complexes Supported by a Bulky Silylamido Ligand Produce Ultra-High-Molecular Weight Polyethylene in the Absence of Activators. *Helv. Chim. Acta* 2016, 99, 859–867.
- (5) Witzke, R. J.; Tilley, T. D. A Two-Coordinate Ni(I) Silyl Complex: CO₂ Insertion and Oxidatively-Induced Silyl Migrations. *Chem. Commun.* **2019**, *55*, 6559–6562.
- (6) Lipschutz, M. I.; Tilley, T. D. Synthesis and Reactivity of a Conveniently Prepared Two-Coordinate Bis(Amido) Nickel(II) Complex. *Chem. Commun.* **2012**, *48*, 7146–7148.
- (7) Lipschutz, M. I.; Tilley, T. D. Useful Method for the Preparation of Low-Coordinate Nickel(I) Complexes via Transformations of the Ni(I) Bis(Amido) Complex $K\{Ni[N(SiMe_3)(2,6-(i)Pr_2-C_6H_3)]_2\}$. Organometallics **2014**, 33, 5566–5570.
- (8) Lipschutz, M. I.; Chantarojsiri, T.; Dong, Y.; Tilley, T. D. Synthesis, Characterization, and Alkyne Trimerization Catalysis of a Heteroleptic Two-Coordinate Fe I Complex. *J. Am. Chem. Soc.* **2015**, 137, 6366–6372.
- (9) Lipschutz, M. I.; Yang, X.; Chatterjee, R.; Tilley, T. D. A Structurally Rigid Bis(Amido) Ligand Framework in Low-Coordinate Ni(I), Ni(II), and Ni(III) Analogues Provides Access to a Ni(III) Methyl Complex via Oxidative Addition. *J. Am. Chem. Soc.* **2013**, *135*, 15298–15301.
- (10) Lipschutz, M. I.; Tilley, T. D. Carbon-Carbon Cross-Coupling Reactions Catalyzed by a Two-Coordinate Nickel(II)-Bis(Amido) Complex via Observable NiI, NiII, and NiIII Intermediates. *Angew. Chem., Int. Ed.* **2014**, 53, 7290–7294.
- (11) Cai, I. C.; Ziegler, M. S.; Bunting, P. C.; Nicolay, A.; Levine, D. S.; Kalendra, V.; Smith, P. W.; Lakshmi, K. V.; Tilley, T. D. Monomeric, Divalent Vanadium Bis(Arylamido) Complexes: Linkage Isomerism and Reactivity. *Organometallics* **2019**, *38*, 1648–1663.
- (12) Hazari, N.; Melvin, P. R.; Beromi, M. M. Well-Defined Nickel and Palladium Precatalysts for Cross-Coupling. *Nat. Rev. Chem.* **2017**, 1, 0025.
- (13) Yang, J.; Tilley, T. D. Efficient Hydrosilylation of Carbonyl Compounds with the Simple Amide Catalyst $[Fe\{N(SiMe_3)_2\}_2]$. Angew. Chem., Int. Ed. **2010**, 49, 10186–10188.
- (14) Sharpe, H. R.; Geer, A. M.; Williams, H. E.; Blundell, T. J.; Lewis, W.; Blake, A. J.; Kays, D. L. Cyclotrimerization of Isocyanates by Low Coordinate Complex. *Chem. Commun.* **2017**, *53*, 937–940.
- (15) Ung, G.; Peters, J. C. Low-Temperature N_2 Binding to Two-Coordinate L_2Fe^0 Enables Reductive Trapping of L_2FeN_2 and NH_3 Generation. *Angew. Chem.* **2015**, 127, 542—545.

- (16) Reppe, W.; Schlichting, O.; Klager, K.; Toepel, T. Cyclisierende Polymerisation von Acetylen I Über Cyclooctatetraen. *Justus Liebigs Ann. Chem.* **1948**, *560*, 1–92.
- (17) Domínguez, G.; Pérez-Castells, J. Recent Advances in [2 + 2+2] Cycloaddition Reactions. *Chem. Soc. Rev.* **2011**, *40*, 3430–3444.
- (18) Link, A.; Sparr, C. Stereoselective Arene Formation. Chem. Soc. Rev. 2018, 47, 3804–3815.
- (19) Chouraqui, G.; Petit, M.; Phansavath, P.; Aubert, C.; Malacria, M. From an Acyclic, Polyunsaturated Precursor to the Polycyclic Taxane Ring System: The [4 + 2]/[2 + 2+2] and [2 + 2+2]/[4 + 2] Cyclization Strategies. European. *Eur. J. Org. Chem.* **2006**, No. 6, 1413—1421.
- (20) Kotha, S.; Sreevani, G. Cyclotrimerization with Propargyl Halides as Copartners: Formal Total Synthesis of the Antitumor Hsp90 Inhibitor AT13387. *ACS Omega* **2018**, *3*, 1850–1855.
- (21) Alayrac, C.; Schollmeyer, D.; Witulski, B. First Total Synthesis of Antiostatin A1, a Potent Carbazole-Based Naturally Occurring Antioxidant. *Chem. Commun.* **2009**, No. 12, 1464–1466.
- (22) McIver, A. L.; Deiters, A. Tricyclic Alkaloid Core Structures Assembled by a Cyclotrimerization coupled Intramolecular Nucleophilic Substitution Reaction. *Org. Lett.* **2010**, *12*, 1288–1291.
- (23) Paymode, D. J.; Ramana, C. V. Total Synthesis of (\pm) -Allocolchicine and Its Analogues Using Co-Catalyzed Alkyne [2 + 2 + 2]-Cyclotrimerization. *ACS Omega* **2017**, 2, 5591–5600.
- (24) More, A. A.; Ramana, C. V. Alkyne [2 + 2 + 2]-Cyclotrimerization Approach for Synthesis of 6,7-Cyclopropylallocolchicinoids. *J. Org. Chem.* **2016**, *81*, 3400–3406.
- (25) Ramana, C. V.; Dushing, M. P.; Mohapatra, S.; Mallik, R.; Gonnade, R. G. Target Cum Flexibility: An Alkyne [2 + 2+2]-Cyclotrimerization Strategy for Synthesis of Trinem Library. *Tetrahedron Lett.* **2011**, 52, 38–41.
- (26) Ramana, C. V.; Salian, S. R.; Gonnade, R. G. An Expeditious Assembly of 3,4-Benzannulated 8-Oxabicyclo[3.2.1]Octane Systems by [2 + 2+2] Alkyne Cyclotrimerisation: Total Synthesis of (–)-Bruguierol A. Eur. J. Org. Chem. 2007, No. 33, 5483–5486.
- (27) Nicolaou, K. C.; Tang, Y.; Wang, J. Total Synthesis of Sporolide B. J. Am. Chem. Soc. **2010**, 132, 11350–11363.
- (28) Aubert, C.; Betschmann, P.; Eichberg, M. J.; Gandon, V.; Heckrodt, T. J.; Lehmann, J.; Malacria, M.; Masjost, B.; Paredes, E.; Vollhardt, K. P. C.; Whitener, G. D. Cobalt-Mediated [2 + 2 + 2] Cycloaddition versus C-H and N-H Activation of Pyridones and Pyrazinones with Alkynes: An Experimental Study. *Chem. Eur. J.* **2007**, 13, 7443—7465.
- (29) Aubert, C.; Gandon, V.; Geny, A.; Heckrodt, T. J.; Malacria, M.; Paredes, E.; Vollhardt, K. P. C. Cobalt-Mediated [2 + 2 + 2] Cycloaddition versus C-H and N-H Activation of 2-Pyridones and Pyrazinones with Alkynes: A Theoretical Study. *Chem. Eur. J.* **2007**, 13, 7466–7478.
- (30) Welsch, T.; Tran, H.; Witulski, B. Total Syntheses of the Marine Illudalanes Alcyopterosin I, L, M, N, and C. *Org. Lett.* **2010**, *12*, 5644–5647.
- (31) Kotha, S.; Lahiri, K.; Sreevani, G. Design and Synthesis of Aromatics through [2 + 2+2] Cyclotrimerization. *Synlett* **2018**, 29, 2342–2361.
- (32) Agenet, N.; Gandon, V.; Vollhardt, K. P. C.; Malacria, M.; Aubert, C. Cobalt-Catalyzed Cyclotrimerization of Alkynes: The Answer to the Puzzle of Parallel Reaction Pathways. *J. Am. Chem. Soc.* **2007**, *129*, 8860–8871.
- (33) Yamamoto, K.; Nagae, H.; Tsurugi, H.; Mashima, K. Mechanistic Understanding of Alkyne Cyclotrimerization on Mononuclear and Dinuclear Scaffolds: [4 + 2] Cycloaddition of the Third Alkyne onto Metallacyclopentadienes and Dimetallacyclopentadienes. *Dalton Trans.* **2016**, *45*, 17072–17081.
- (34) Kwon, D. H.; Proctor, M.; Mendoza, S.; Uyeda, C.; Ess, D. H. Catalytic Dinuclear Nickel Spin Crossover Mechanism and Selectivity for Alkyne Cyclotrimerization. *ACS Catal.* **2017**, *7*, 4796–4804.
- (35) Hollingsworth, R. L.; Bheemaraju, A.; Lenca, N.; Lord, R. L.; Groysman, S. Divergent Reactivity of a New Dinuclear Xanthene-

- Bridged Bis(Iminopyridine) Di-Nickel Complex with Alkynes. *Dalton Trans.* **2017**, *46*, 5605–5616.
- (36) Yamamoto, K.; Tsurugi, H.; Mashima, K. Direct Evidence for a [4+2] Cycloaddition Mechanism of Alkynes to Tantallacyclopentadiene on Dinuclear Tantalum Complexes as a Model of Alkyne Cyclotrimerization. *Chem. Eur. J.* **2015**, *21*, 11369–11377.
- (37) Duong, H. A.; Tekavec, T. N.; Arif, A. M.; Louie, J. Reversible Carboxylation of N-Heterocyclic Carbenes. *Chem. Commun.* **2004**, 112–113.
- (38) Thomas, R.; Lakshmi, S.; Pati, S. K.; Kulkarni, G. U. Role of Triple Bond in 1,2-Diphenylacetylene Crystal: A Combined Experimental and Theoretical Study. *J. Phys. Chem. B* **2006**, *110*, 24674—24677.
- (39) Riener, K.; Haslinger, S.; Raba, A.; Högerl, M. P.; Cokoja, M.; Herrmann, W. A.; Kühn, F. E. Chemistry of Iron N -Heterocyclic Carbene Complexes: Syntheses, Structures, Reactivities, and Catalytic Applications. *Chem. Rev.* **2014**, *114*, 5215–5272.
- (40) Laskar, P.; Yamamoto, K.; Nishi, K.; Ikeda, H.; Tsurugi, H.; Mashima, K. C_{β} - C_{β} Bond Fission of Metallacyclopentadiene over a Low-Valent Ditantalum Scaffold. *Organometallics* **2019**, 38, 722–729.
- (41) Reiff, W. M.; LaPointe, A. M.; Witten, E. H. Virtual Free Ion Magnetism and the Absence of Jahn-Teller Distortion in a Linear Two-Coordinate Complex of High-Spin Iron(II). *J. Am. Chem. Soc.* **2004**, 126, 10206–10207.
- (42) Zadrozny, J. M.; Xiao, D. J.; Long, J. R.; Atanasov, M.; Neese, F.; Grandjean, F.; Long, G. J. Mössbauer Spectroscopy as a Probe of Magnetization Dynamics in the Linear Iron(I) and Iron(II) Complexes $[Fe(C(SiMe_3)_3)_2]^{1-/0}$. *Inorg. Chem.* **2013**, *52*, 13123–13131.
- (43) Mardirossian, N.; Head-Gordon, M. ω b97X-V: A 10-Parameter, Range-Separated Hybrid, Generalized Gradient Approximation Density Functional with Nonlocal Correlation, Designed by a Survival-of-the-Fittest Strategy. *Phys. Chem. Chem. Phys.* **2014**, *16*, 9904–9924.
- (44) Huang, Y.-S.; Huang, G.-T.; Liu, Y.-L.; Yu, J.-S. K.; Tsai, Y.-C. Reversible Cleavage/Formation of the Cr-Cr Quintuple Bond in the Highly Regioselective Alkyne Cyclotrimerization. *Angew. Chem., Int. Ed.* **2017**, *56*, 15427–15431.
- (45) Mardirossian, N.; Head-Gordon, M. Thirty Years of Density Functional Theory in Computational Chemistry: An Overview and Extensive Assessment of 200 Density Functionals. *Mol. Phys.* **2017**, *115*, 2315–2372.
- (46) Goerigk, L.; Hansen, A.; Bauer, C.; Ehrlich, S.; Najibi, A.; Grimme, S. A Look at the Density Functional Theory Zoo with the Advanced GMTKN55 Database for General Main Group Thermochemistry, Kinetics and Noncovalent Interactions. *Phys. Chem. Chem. Phys.* 2017, 19, 32184–32215.
- (47) Chan, B.; Gill, P. M. W.; Kimura, M. Assessment of DFT Methods for Transition Metals with the TMC151 Compilation of Data Sets and Comparison with Accuracies for Main-Group Chemistry. *J. Chem. Theory Comput.* **2019**, *15*, 3610–3622.
- (48) Marquard, S. L.; Bezpalko, M. W.; Foxman, B. M.; Thomas, C. M. Stoichiometric C=O Bond Oxidative Addition of Benzophenone by a Discrete Radical Intermediate to Form a Cobalt(I) Carbene. *J. Am. Chem. Soc.* **2013**, *135*, 6018–6021.
- (49) Parmelee, S. R.; Mazzacano, T. J.; Zhu, Y.; Mankad, N. P.; Keith, J. A. A Heterobimetallic Mechanism for C-H Borylation Elucidated from Experimental and Computational Data. *ACS Catal.* **2015**, *5*, 3689–3699.